Probabilistic Seismic Demand Analysis Using Improved Intensity Measures

L. Lin
Concordia University, Canada

SUMMARY:
Probabilistic seismic demand analysis (PSDA) is one of the main phases in the framework methodology for performance-based earthquake engineering. For a given structure, PSDA is used to determine the mean annual frequencies of exceeding specified values of a structural response parameter due to future earthquake motions. This is done by combining the seismic hazard at the location of the structure and the structural response obtained from nonlinear dynamic analysis for a selected set of earthquake records. The spectral acceleration at the fundamental structural period ($Sa(T_1)$) is the most widely used intensity measure. Very recently, two improved intensity measures were developed, i.e., S_{N1} – for short- and intermediate period buildings, and S_{N2} – for long-period buildings. This paper describes the formulation and development of these two intensity measures. The application of the developed intensity measures is also presented in this paper. The analyses showed that the use of the intensity measures S_{N1} and S_{N2} leads to lower seismic demands relative to those corresponding to $Sa(T_1)$, especially for long-period buildings.

Keywords: seismic, intensity measure, interstorey drift, reinforced concrete building, standard deviation.

1. INTRODUCTION

Probabilistic seismic demand analysis (PSDA) is an important phase of the new approach for seismic assessment of existing structures and design of new structures, known as performance-based earthquake engineering (PBEE) (Cornell and Krawinkler 2000; Moehle and Deierlein 2004). The goal of PSDA for a given structure is to compute the mean annual frequencies of exceeding specified levels of structural response due to future seismic motions that might occur at the location of the structure. This is done by combining the seismic hazard at the location of the structure considered, and the response of the structure subjected to seismic motions scaled to a range of intensity levels. In PSDA, the structural response is represented by an engineering demand parameter (*EDP*), and the ground motion intensity is represented by an intensity measure (*IM*) (Moehle and Deierlein 2004).

In this study, the maximum interstorey drift over the height of the building structures, obtained from nonlinear dynamic analyses, is used as *EDP*. It is a 'global' response parameter and is used in code-related documents as an indicator of damage to structures due to seismic motions (ASCE 2000; Vision 2000 Committee 1995). In general, it is known that interstorey drift correlates well with structural damage, and it is the most used parameter for investigation of the seismic vulnerability of buildings (Moehle 1984; Miranda and Akkar 2006; Bozorgnia and Bertero 2001).

The other parameter in PSDA, i.e., the intensity measure (*IM*), is used for scaling the records in the computation of the responses of the structure considered. The scaling is conducted to a series of *IM* levels in order to produce a representative range of cases of the structural behaviour due to future earthquakes, i.e., from elastic responses to collapse. Currently, spectral acceleration at the first mode period ($Sa(T_1)$) is the most used *IM*. It is known, however, that $Sa(T_1)$ has significant deficiencies when used as *IM*. Namely, $Sa(T_1)$ does not include the effects of the period elongation during nonlinear response and the contribution of the higher modes to the structural response. Given this, comprehensive research has been conducted in recent years, and several new intensity measures have been developed. For example, Cordova et al. (2001) introduced an *IM* that takes into account the elongation of the first mode period during nonlinear response. The analysis results showed that this *IM* is more effective than $Sa(T_1)$. However, given the limited investigations (for composite and steel frames, and small number of records), further research is needed for this *IM*, specifically for reinforced concrete buildings and using larger sets of records. Baker and Cornell (2005) proposed an *IM* that consists of two parameters – the spectral acceleration at the first mode period ($Sa(T_1)$), and 'epsilon' (ε). The parameter ε is defined by engineering seismologists studying ground motions as a measure of the difference between the spectral acceleration of a record and the spectral acceleration from an attenuation relation at the given period. This *IM* has not been used in practical applications primarily because structural engineers are not familiar with ε, and this parameter is not readily available for recorded motions. Luco and Cornell (2007) developed an *IM* called $IM_{1I\&2E}$, where *1I* designates 1st mode-Inelastic, and *2E* designates 2nd mode-Elastic. It has been found that $IM_{1I\&2E}$ is effective for predicting the maximum drift response. However, the use of $IM_{1I\&2E}$ is presently limited to research because the attenuation relation which is needed for PSDA is not available for this *IM*.

It is seen from this review that advanced *IMs* are available for PSDA, but they are currently not used in practice because of different limitations, as discussed above. The objective of this study is to develop improved intensity measures that are effective for predicting structural responses and are easy for use in PSDA. This was done by investigating the seismic responses of three reinforced concrete frame buildings (4-, 10-, and 16-storey high) subjected to a selected set of records scaled to different intensity levels.

2. DESCRIPTION OF BUILDINGS

Three reinforced concrete frame buildings were used in this study (Fig. 2.1). The buildings are for office use and are located in Vancouver, which is in a high seismic hazard zone (NRCC 2005). The buildings are identical in plan but have different heights. As shown in Fig. 2.1, the buildings include a 4-storey, a 10-storey, and a 16-storey building, which are considered representative of low-rise, medium-rise and high-rise buildings, respectively.

The plan of each building is 27.0 m x 63.0 m. The storey heights are 3.65 m. The lateral load resisting system consists of moment-resisting reinforced concrete frames in both the longitudinal and the transverse directions. There are four frames in the longitudinal direction (designated *Le* and *Li* in Fig. 2.1; *Le* – exterior frames, and *Li* – interior frames) and eight frames in the transverse direction (*Te* and *Ti*). The distance between both the longitudinal and the transverse frames is 9.0 m. Secondary beams between the longitudinal frames are used at the floor levels in order to reduce the depth of the floor slabs. The secondary beams are supported by the beams of the transverse frames. The floor system consists of a one-way slab spanning in the transverse direction, supported by the beams of the longitudinal frames and the secondary beams. The slab is cast integrally with the beams.

In this study, only the interior transverse frames (*Ti*) of the buildings were considered. For ease of discussion, the 4-storey, the 10-storey, and the 16-storey frames are referred to as the 4S, the 10S, and the 16S frames, respectively. The frames were designed as *ductile* reinforced concrete frames in accordance with the National Building Code of Canada (NBCC) (NRCC 2005). The foundations were assumed to be on stiff soil represented by site class C in NBCC (shear wave velocity between 360 m/s and 750 m/s).

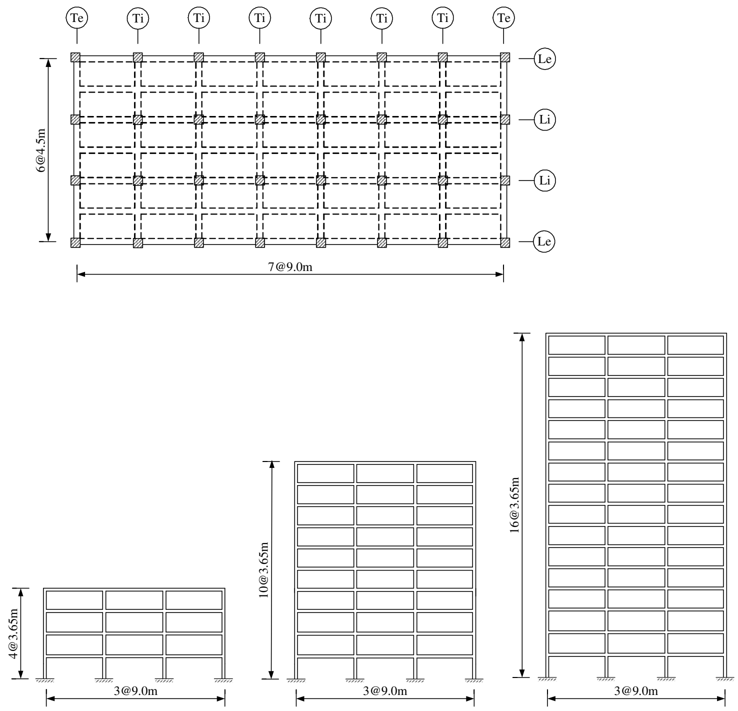

Figure 2.1. Plan of floors and elevations of transverse frames of the buildings

3. MODELING OF FRAMES FOR DYNAMIC ANALYSIS

Inelastic models of the frames were developed for use in the two-dimensional (2D) inelastic dynamic analysis program RUAUMOKO (Carr 2004). The beams and the columns were modelled by a 'beam-column' element, which is represented by a single component flexural spring. Inelastic deformations are assumed to occur at the ends of the element where plastic hinges can be formed. The effects of axial deformations in beams are neglected. Axial deformations are considered for columns, but no interaction between bending moment and axial load is taken into account. It is necessary to mention that a trilinear hysteretic model was selected for modeling columns, and a bilinear (modified Takeda) model was selected for modeling beams. Both models take into account the degradation of the stiffness during nonlinear response. The natural periods of the first two vibration modes of the frames, obtained by RUAUMOKO, are given in Table 3.1. These were used in the development of the new intensity measures, as discussed below in this paper.

Table 3.1. Natural periods of the frame models (in seconds)

Frame model	Mode No.	
	1	2
4S	0.94	0.29
10S	1.96	0.70
16S	2.75	1.02

4. FORMULATION OF IMPROVED INTENSITY MEASURES

A preferable intensity measure (*IM*) would be one that: (i) takes into account the effects of at least the first and the second modes of vibration, and (ii) includes the effects of the period elongation during nonlinear response. Using spectral acceleration (*Sa*) as a response parameter, an *IM* (designated S_N, where *N* stands for 'new') that satisfies these requirements can be expressed in a general form as (Lin 2008):

$$S_N = Sa(T_1)^{\alpha} \times Sa(T_2)^{\beta} \times Sa(T_f)^{\gamma} \tag{4.1}$$

where T_1 and T_2 are elastic periods of the first and the second modes, respectively, and T_f is the lengthened period of the first mode. The exponents α, β, and γ are intended to represent the 'weights' of the contributions of $Sa(T_1)$, $Sa(T_2)$, and $Sa(T_f)$, respectively, to the structural response. The sum of the weights must be 1. Note that the exponents in Eq. 4.1 and in similar equations in the rest of this paper, apply to the *Sa* values for the specific periods, and not to the periods in brackets. While this would be an efficient *IM*, it is difficult to derive such an *IM* because of the complexity associated with the determination of the parameters α, β, γ, and T_f. Even for a single structure, thousands of time-history analyses are required to determine optimum values for these parameters.

To simplify the problem, the issues on the period elongation and the second mode effects in this study were considered separately. Two *IMs*, denoted S_{N1} and S_{N2}, were investigated in this paper. The intensity measure S_{N1} takes into account the first mode vibrations and the elongation of the first mode period, whereas S_{N2} takes into account the first and the second mode vibrations. These are expressed as follows:

$$S_{N1} = Sa(T_1)^{\alpha} \times Sa(CT_1)^{1-\alpha} \tag{4.2}$$

$$S_{N2} = Sa(T_1)^{\beta} \times Sa(T_2)^{1-\beta} \tag{4.3}$$

It can be seen in Eq. 4.2 that the elongated period is expressed as a product of the elastic first mode period T_1 and a constant C, i.e., $T_f = C{\cdot}T_1$. Note that the term $C{\cdot}T_1$ used in the intensity measure S_{N1} represents a significant approximation of the period elongation. Equations. 4.2 and 4.3 are based on the assumption that the response of a specific structure is dominated exclusively either by the first mode effects and the period elongation of that mode, or by the first and the second mode effects.

5. ANALYSIS OF THE INTENSITY MEASURES S_{N1} and S_{N2}

5.1 Intensity Measure S_{N1} - Effects of Period Elongation

To determine the optimal values for the coefficients C and α included in S_{N1} (Eq. 4.2), 'trial' values for the coefficients were selected for use in the analysis. These included:

- C = 1.5, and 2.0,
- α = 0.25, 0.50, and 0.75.

The 'trial' values for C were chosen based on results from an investigation of the first mode period elongation of the 4S, the 10S and the 16S frames subjected to the selected set of records (Lin 2008). This investigation showed that when the lengthened period was longer than about twice the elastic period (i.e., $C \geq 2.0$), most of the records caused collapse of the frames. Based on this, the value of C = 2.0 was selected as an upper limit for C. The other 'trial' value, i.e., C = 1.5, was chosen to be in the middle between the upper limit (C = 2.0) and C = 1.0 which corresponds to elastic response. Note that C = 1.5 is used in the ASCE/SEI 7-05 Standard (ASCE 2006) as a period elongation factor.

Optimal values for the coefficients C and α were considered those that provide the smallest dispersions (i.e., standard deviations) of the maximum interstorey drifts (*IDR*s) obtained from dynamic analyses of the frames using S_{N1} as *IM*. The dispersion (σ_{lnIDR}) was considered because it is an indicator of the efficiency of an intensity measure (Tothong and Cornell 2007).

To compare the dispersions of the *IDRs* associated with S_{N1} and $Sa(T_1)$, nonlinear time history analyses were conducted on the 4S, 10S, and 16S frames subjected to a set of 20 records using the intensity measures S_{N1} and $Sa(T_1)$, respectively. The results from the analyses show that for the 4S frame, the smallest σ_{lnIDR} values correspond to C = 1.5 and α = 0.50. Overall, the dispersion of the interstorey drifts for the 4S frame resulting from the use of S_{N1} with C = 1.5 and α = 0.50 is about 40% to 50% smaller than that resulting from the use of $Sa(T_1)$ as *IM*. However the results for the 10S and the 16S frames show that the use of S_{N1} as *IM* produces a slight reduction (about 15%) in the σ_{lnIDR} results for few α values used with C = 1.5, and almost no reduction for the cases with C = 2.0.

Using the optimal coefficients C = 1.5 and α = 0.50, the intensity measure S_{N1} (Eq. 4.2) can be expressed as:

$$S_{N1} = Sa(T_1)^{0.5} \times Sa(1.5T_1)^{0.5} \tag{4.4}$$

5.2 Intensity Measure S_{N2} - Effects of the Second Mode

The procedure for determining the optimal value for the coefficient β used in S_{N2} is the same as that applied in the investigation of the intensity measure S_{N1}, except that only one coefficient (i.e., β) is required to be determined. The selected 'trial' values for β were 0.50, 0.75, and 0.85. The elastic periods of the first and second modes are given in Table 3.1.

Based on the results from the analyses, it was found that for the 10S and the 16S frames, the smallest σ_{lnIDR} values correspond to β = 0.75. Therefore, β = 0.75 is considered as optimal value for these frames. The σ_{lnIDR} values for S_{N2} with β = 0.75 are about 30% smaller than the values for $Sa(T_1)$. This indicates that the second mode has significant contributions to the responses of the 10S and the 16S frames, and the new intensity measure S_{N2} with β = 0.75 is efficient for these frames. However, for the 4S frame, the σ_{lnIDR} values for β = 0.75 and β = 0.85 are slightly smaller than those obtained for $Sa(T_1)$. The maximum difference is only about 7%, which is not of importance for practical applications. Note that the σ_{lnIDR} values for β = 0.50 are even larger than those obtained for $Sa(T_1)$. This shows that S_{N2} as *IM* is not efficient for the 4S frame compared to $Sa(T_1)$. It is mainly because the second mode effects for the 4S frame are quite small, i.e., the response of the frame is dominated by the first mode.

Using the value for β = 0.75, Eq. 4.3 is written as:

$$S_{N2} = Sa(T_1)^{0.75} \times Sa(T_2)^{0.25} \tag{4.5}$$

6. PROBABILISTIC SEISMIC DEMAND ANALYSIS USING IMPROVED INTENSITY MEASURES

Probabilistic seismic demand analysis (PSDA) is an approach for the calculation of the mean annual frequencies of exceeding given structural response levels due to seismic motions. The two major quantities used in PSDA of a given structure are (i) the structural response due to seismic motions and (ii) the intensity of the motions. In PSDA, the structural response is represented by an engineering demand parameter (*EDP*), and the intensity of the seismic motions is represented by an intensity measure (*IM*) (e.g., $Sa(T_1)$). In this study, maximum interstorey drift (*IDR*) is used as *EDP*, and the proposed intensity measures S_{N1} and S_{N2} (Eqs. 4.4 and 4.5) are used as *IMs*. Using this terminology, the mean annual frequency of exceeding a given *IDR* level *idr*, designated $\lambda_{IDR}(idr)$, is calculated as (Baker and Cornell 2005):

$$\lambda_{IDR}(idr) = \int_{im} P(IDR > idr \mid IM = im) \times \left| \frac{d\lambda_{IM}(im)}{d(im)} \right| d(im) \tag{4.6}$$

Note that $\lambda_{IDR}(idr)$ is also referred to as the drift (or the demand) hazard curve. It is seen from Eq. 4.6 that PSDA requires the computation of the structural response (*IDRs*) and the seismic hazard ($\lambda_{IM}(im)$). It is necessary to mention that Eq. 4.6 is expressed using general designation for the intensity measure (i.e., *IM*) not the two new intensity measures S_{N1} and S_{N2} developed in this study.

6.1 Maximum *IDR*s

The responses of the frame models were computed using nonlinear time-history analysis for excitation motions represented by the selected set of 80 records. The computer program RUAUMOKO (Carr

2004) was used for the dynamic analyses of the frames. To determine the maximum *IDRs* due to ground motions with different intensities, the records were scaled to a range of intensity levels. The 4S frame was analysed for scaled records based on $IM = S_{N1}$, while the 10S and 16S frames were analysed for $IM = S_{N2}$. Fourteen intensity levels were considered for each frame. For illustration, Fig. 6.2 shows the computed maximum *IDR* values for the 10S frame for records scaled to $IM = S_{N2}$. Each stripe of points in the figure represents the *IDRs* for the 80 records used in the analysis, scaled to a given intensity level. In general, *IDR* values of the order of 15% and above were obtained for the largest excitation levels. Certainly, such large *IDRs* cannot be resisted by the frames, i.e., the frames would collapse when their *ultimate* capacities (i.e., collapse drift limits) are exceeded. Since the program RUAUMOKO does not identify the collapse, an estimate of the ultimate drift capacities of the frames is needed in order to determine which records cause collapse. In this study, the collapse was defined to occur if the *IDR* obtained from the dynamic analysis exceeds 5%. The selection of the value of 5% as ultimate drift for the frames analysed in this study is discussed in detail in Lin (2008).

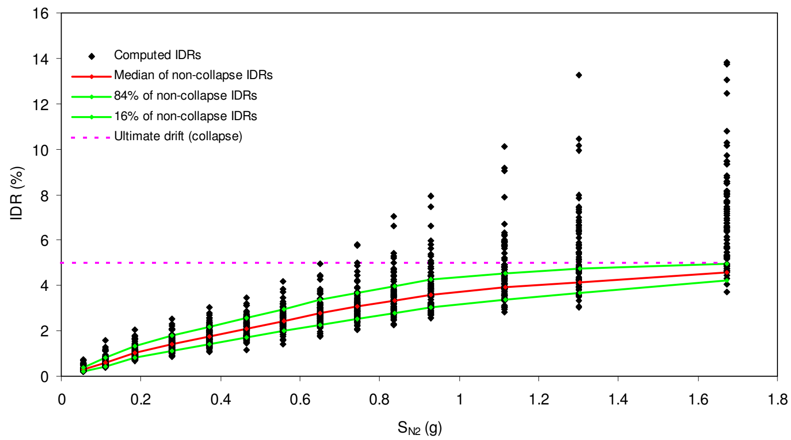

Figure 6.2. Computed maximum interstorey drifts for the 10S frame using S_{N1} as *IM*

To calculate the probability $P(IDR>idr|IM=im)$, one should consider both the *IDRs* that are below the 5% ultimate drift (referred to as non-collapse *IDRs*) and those that exceed the ultimate drift (referred to as the collapses) (Fig. 6.2). Non-collapse *IDRs* at a given excitation level have been found to follow lognormal distribution (Baker and Cornell 2005). For such distribution, the conditional probability of the non-collapse *IDRs* can be expressed as:

$$P(IDR > idr \mid IM = im, non-collapse) = 1 - \Phi\left(\frac{(\ln idr \mid IM = im) - \mu_{\ln IDR|IM=im}}{\sigma_{\ln IDR|IM=im}}\right) \tag{4.7}$$

where $\Phi(\bullet)$ denotes the standard normal cumulative distribution function.

The calculation of the probability of collapse was done as suggested by Baker and Cornell (2005). According to their method, the calculations of the collapse probabilities $P(C|IM=im)$ for a given frame was simply done by counting the collapses for each $IM = im$, and expressing these as a fraction of the total number of responses.

The probabilities of the non-collapse (Eq. 4.7) and the collapse results defined above (were combined using the total probability theorem. The probability that *IDR* exceeds a specified value *idr* for a given $IM = im$ is expressed as:

$$P(IDR > idr \mid IM = im) = P(C \mid IM = im) + \\ [1 - P(C \mid IM = im)] \cdot \left[1 - \Phi(\frac{\ln idr - \mu_{\ln IDR|IM=im}}{\sigma_{\ln IDR|IM=im}})\right] \tag{4.8}$$

6.2 Seismic Hazard

6.2.1 Mean attenuation relations

To simplify the derivations of the attenuation relations for the intensity measures S_{N1} and S_{N2}, a general intensity measure, *IM*, is introduced to represent both S_{N1} and S_{N2}. Based on Eqs. 4.4 and 4.5, the intensity measures S_{N1} and S_{N2} can be expressed in a general form as:

$$IM = Sa(T_1)^x \cdot Sa(T_z)^y \tag{4.9}$$

In Eq. 4.9, *IM* stands for S_{N1} or S_{N2}, T_z stands for $1.5T_1$ or T_2, whereas x and y represent the exponents in Eqs. 4.4 and 4.5. Note that T_1 and T_2 are the first and the second mode periods of the frames. Equation 4.9 is introduced to generalise the derivations of the parameters required for the mean attenuation relations for S_{N1} and S_{N2}. Expressed in natural logarithms, Eq. 4.9 has the form:

$$\ln IM = x \ln Sa(T_1) + y \ln Sa(T_z) \tag{4.10}$$

As seen in Eq. 4.10, the attenuation relations for the new intensity measures *IM* (i.e., S_{N1} and S_{N2}) can be determined based on available attenuation relations for spectral accelerations.

6.2.2 Standard deviations

Standard deviations for the attenuation relations for S_{N1} and S_{N2} are also needed for conducting seismic hazard analysis. For ease of discussion, a general intensity measure, *IM*, representing both S_{N1} and S_{N2} (Eq. 4.9) is used again here. In order to determine the standard deviation for *IM*, the correlation coefficients of the spectral accelerations $Sa(T_1)$ and $Sa(T_z)$ involved in *IM* (Eq. 4.9) are needed to define.

Investigations of the correlation of spectral accelerations at two periods have been conducted by Inoue and Cornell (1990) and Baker and Cornell (2006) for earthquake motions recorded in California. The equations for correlation coefficients resulting from these investigations provide very similar results. In this paper, the equation proposed by Inoue and Cornell (1990) was used, primarily because of its simplicity. The correlation coefficient for the natural logarithms of the spectral accelerations at periods T_1 and T_z, as formulated in Inoue and Cornell (1990), can be expressed as:

$$\rho_{\ln Sa(T_1),Sa(T)_z} = 1 - 0.33\left|\ln\left(T_z / T_1\right)\right| \tag{4.11}$$

Now the standard deviation of *lnIM* can be written as:

$$\sigma^2_{\ln_{IM}} = x^2\sigma^2_{\ln Sa(T_1)} + y^2_{\ln Sa(T_z)} + 2\rho_{\ln Sa(T_1),\ln Sa(T_z)} xy\sigma_{\ln Sa(T_1)}\sigma_{\ln Sa(T_2)} \tag{4.12}$$

The correlation coefficients and the standard deviations for S_{N1} and S_{N2} can now be calculated by substituting into Eqs. 4.11 and 4.12 the corresponding values for T_1, T_z, x, y, $\sigma_{\ln Sa(T1)}$, and $\sigma_{\ln Sa(Tz).}$

By conducting probabilistic seismic hazard analysis, the seismic hazard curves with respect to $IM = S_{N1}$ and $IM = S_{N2}$, were computed for the 4S, the 10S, and the 16S frames (Fig. 6.3), based on the seismic conditions for Vancouver (for which the frames were designed) and the attenuation relations developed for S_{N1} and S_{N2}. Note that the seismic hazard curve for the 4S frame was determined using the intensity measure S_{N1}, and those for the 10S and the 16S frames were obtained using S_{N2}. The hazard analyses were conducted by Geological Survey of Canada (Adams and Halchuk, personal communication, 2006).

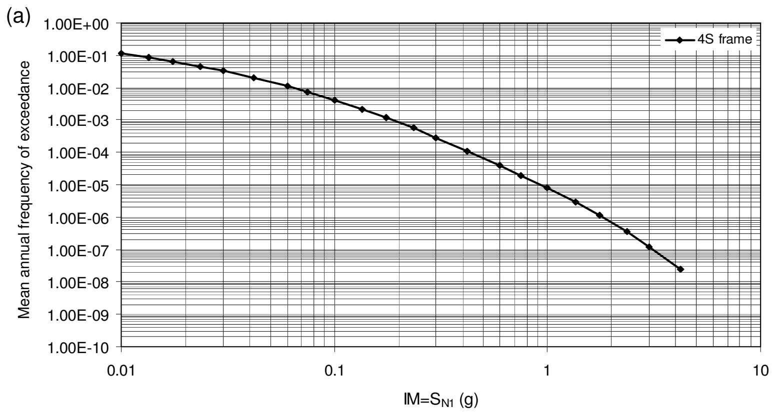

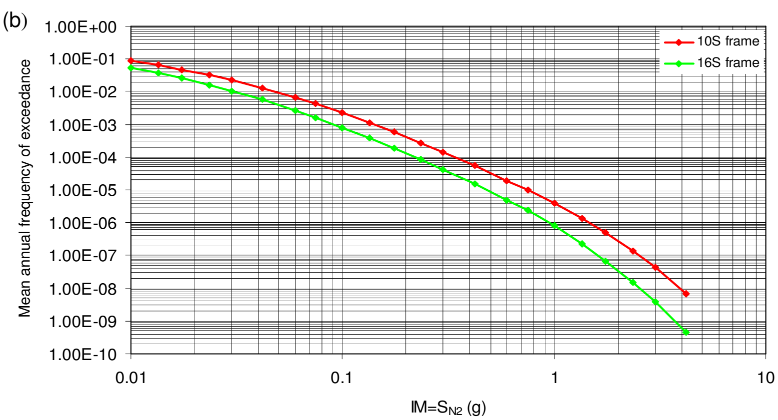

Figure 6.3. Seismic hazard curves: (a) for the 4S frame ($IM = S_{N1}$), (b) for the 10S and 16S frames ($IM = S_{N2}$)

6.3 Drift Hazard Curves

The final phase of PSDA is the computation of the drift hazard curves for the frames (designated $\lambda_{IDR}(idr)$ in Eq. 4.6), which represent the mean annual frequencies of exceeding specified interstorey drift (IDR) levels idr. The computation was conducted using Eq. 4.6 with the combination of Eqs. 4.8, 4.10 to 4.13.

Figure 6.4 shows the drift hazard curves based on the intensity measures S_{N1} (for the 4S frame) and S_{N2} (for the 10S and 16S frames). For comparison, the drift hazard curves based on the intensity measure of the spectral acceleration at the first mode period $Sa(T_1)$ are also shown in Fig. 6.4. It can be seen in Fig. 6.4 that the differences between the drift hazard curves corresponding to S_{N1} and $Sa(T_1)$ are relatively small for the 4S frame (Fig. 6.4(a)). However, the differences are much larger for the 10S and the 16S frames (Figs. 6.4(b) and 6.4(c)). The maximum difference is about 35% for the 4S frame, 60% for the 10S frame, and 85% for the 16S frame. Note that for both 10S and 16S frames, the drift hazard curves for S_{N2} are significantly lower than those for $Sa(T_1)$.

While the differences observed in Fig. 6.4 are quite large (especially for the 10S and the 16S frames), they were not surprising given the results from other similar studies. Tothong and Cornell (2007) investigated the effects of advanced intensity measures on the drift hazard curves for a number of frame models with different fundamental periods. They reported that the advanced intensity measures produced significantly different drift hazard values compared to those obtained using $Sa(T_1)$ as intensity measure. Differences of up to 90% have been observed. It is useful to mention that in almost all the cases, the drift hazard results from the use of the advanced intensity measures have been found to be smaller than those obtained using $Sa(T_1)$, as seen in Figs. 6.4(b) and 6.4(c) for the 10S and the 16S frames, respectively. This indicates that the use of the conventional intensity measure, $Sa(T_1)$, might lead to very conservative results relative to the results based on improved intensity measures.

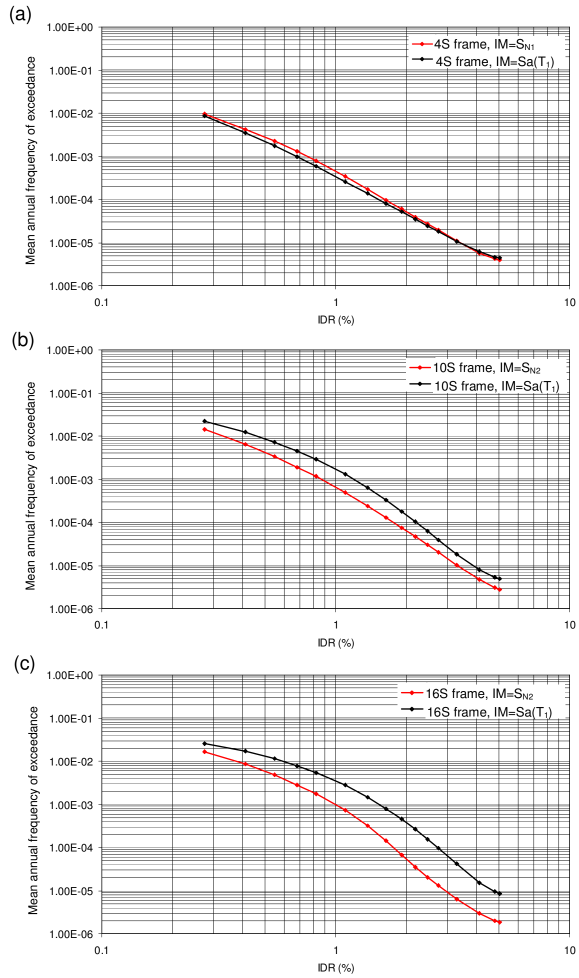

Figure 6.4. Comparison of drift hazard curves obtained using the improved intensity measures S_{N1} and S_{N2} with those obtained using $Sa(T_1)$ for: (a) the 4S frame, (b) the 10S frame, and (c) the 16S frame

7. CONCLUSIONS

This paper presents the development of the new intensity measures and its application in probabilistic seismic demand analysis. For the purpose of the study, three reinforced concrete frame buildings were designed. They are 4-storey, 10-storey and 16-storey buildings. The buildings are located in Vancouver. Two intensity measures, i.e., S_{N1} and S_{N2} were developed in this study. The intensity measure S_{N1} takes into account the effects of the period elongation, and it is intended for use for short- and intermediate-period buildings (e.g., 4S frame in this study). The intensity measure S_{N2} takes into account the second mode effect, and it is intended for use for the long-period buildings (e.g., 10S and 16S frames in this study). The significant advantage of the intensity measures S_{N1} and S_{N2} developed in this study compared with those developed before is the attenuation relations for S_{N1} and S_{N2} can be derived very easily based on the current attenuation relations for spectral accelerations.

The application of the new intensity measures S_{N1} and S_{N2} is illustrated by conducting probabilistic seismic demand analysis on the 4-storey, 10-storey and 16-storey buildings. For the purpose of comparison, probabilistic seismic demand analyses were also carried out by using the spectral acceleration at the fundamental structural period ($Sa(T_1)$) as intensity measure, which is currently the most used intensity measure in practice. It was found that the results from probabilistic seismic demand analysis corresponding to the proposed intensity measures S_{N1} and S_{N2} are significantly different from those obtained using $Sa(T_1)$ as intensity measure, especially for the 10-storey and the 16-storey frames. The maximum differences are about 35% for the 4-storey frame, 60% for the 10-storey frame, and 85% for the 16-storey frame.

In summary, the use of the proposed intensity measures S_{N1} and S_{N2} in probabilistic seismic demand analysis is quite straightforward and provides reliable results. The parameters involved in S_{N1} and S_{N2} are readily available to engineers. The attenuation relations for S_{N1} and S_{N2} can be easily developed based on existing attenuation relations for spectral accelerations. Given this, there are no constraints regarding the application of S_{N1} and S_{N2}, and these intensity measures are recommended for use in probabilistic seismic demand analysis of reinforced concrete frame buildings.

REFERENCES

ASCE. (2006). Minimum design loads for buildings and other structures. *Standard ASCE/SEI 7-05*, American Society of Civil Engineers, Danvers, Massachusetts.

ASCE. (2000). Prestandard and commentary for the seismic rehabilitation of buildings. *Report FEMA 356*, American Society of Civil Engineers, Reston, Virginia.

Baker, J.W., and Cornell, C.A. (2006). Correlation of response spectral values for multicomponent ground motions. *Bulletin of the Seismological Society of America*, **96(1):** 215-227.

Baker, J.W., and Cornell, C.A. (2005). A vector-valued ground motion intensity measure consisting of spectral acceleration and epsilon. *Earthquake Engineering and Structural Dynamics*, **34:** 1193-1217.

Bozorgnia, Y., and Bertero, V.V. (2001). Improved shaking and damage parameters for post-earthquake applications. Proceedings, Strong Motion Instrumentation Program (SMIP01) Seminar on Utilization of Strong-Motion Data, California Division of Mines and Geology, Los Angeles, Calif. pp. 1–22.

Carr, A.J. (2004). RUAUMOKO – Inelastic dynamic analysis program. Department of Civil Engineering, University of Canterbury, Christchurch, New Zealand.

Cordova, P.P., Deierlein, G.G., Mehanny, S.S.F., and Cornell, C.A. (2001). Development of two-parameter seismic intensity measure and probabilistic assessment procedure. *The Second U.S. – Japan Workshop on Performance-based Earthquake Engineering Methodology for Reinforced Concrete Building Structures*, Sapporo, Japan, 187-206.

Cornell, C.A., and Krawinkler, H. (2000). Progress and challenges in seismic performance assessment. *PEER Center News*, 3(2), 4 p. http://peer.berkeley.edu/news/2000spring/performance.html (accessed May 2006).

Inoue, T., and Cornell, C.A. (1990). Seismic hazard analysis of multi-degree-of-freedom structures. Reliability of Marine Structures, *Report RMS-8*, Stanford University, Stanford, CA, 70 p.

Lin, L. (2008). Development of improved intensity measures for probabilistic seismic demand analysis. *PhD thesis*, Department of Civil Engineering, University of Ottawa, Ottawa, Ontario, Canada, 150 p.

Luco, N., and Cornell, C.A. (2007). Structure-specific scalar intensity measure for near-source and ordinary earthquake motions. *Earthquake Spectra*, **23(2):** 357-391.

Miranda, E., and Akkar, S.D. (2006). Generalized interstorey drift spectrum. *Journal of Structural Engineering*, **132(6):** 840–852.

Moehle, J.P. (1984). Strong motion drift estimates for R/C structures. *Journal of Structural Engineering*, **110(9):** 1988–2001.

Moehle, J., and Deierlein, G.G. (2004). A framework methodology for performance-based earthquake engineering. *13th World Conference on earthquake Engineering*, Vancouver, B.C., Canada, on CD-ROM, 13 p.

NRCC. 2005. National Building Code of Canada (2005). Institute for Research in Construction, *National Research Council of Canada*, Ottawa, Ontario, Canada.

Tothong, P., and Cornell, C.A. (2007). Probabilistic seismic demand analysis using advanced ground motion intensity measures, attenuation relationships, and near-fault effects. *PEER Report 2006/11*, Pacific Earthquake Engineering Research Center, University of California, Berkeley, Calif.

Vision 2000 Committee. (1995). Performance based seismic engineering of buildings. *Structural Engineers Association of California (SEAOC)*, San Francisco, CA.